

# ChemComm

Accepted Manuscript



This is an *Accepted Manuscript*, which has been through the Royal Society of Chemistry peer review process and has been accepted for publication.

*Accepted Manuscripts* are published online shortly after acceptance, before technical editing, formatting and proof reading. Using this free service, authors can make their results available to the community, in citable form, before we publish the edited article. We will replace this *Accepted Manuscript* with the edited and formatted *Advance Article* as soon as it is available.

You can find more information about *Accepted Manuscripts* in the [Information for Authors](#).

Please note that technical editing may introduce minor changes to the text and/or graphics, which may alter content. The journal's standard [Terms & Conditions](#) and the [Ethical guidelines](#) still apply. In no event shall the Royal Society of Chemistry be held responsible for any errors or omissions in this *Accepted Manuscript* or any consequences arising from the use of any information it contains.

## COMMUNICATION

# Primary hepatocytes imaging by multiphoton luminescent graphene quantum dots

Cite this: DOI: 10.1039/x0xx00000x

Received 00th January 2012,

Accepted 00th January 2012

DOI: 10.1039/x0xx00000x

www.rsc.org/

Sung Ho Song<sup>a</sup>, Min-Ho Jang<sup>b</sup>, Jong-Min Jeong<sup>c</sup>, Hyewon Yoon<sup>a</sup>, Yong-Hoon Cho<sup>b</sup>, Won-Il Jeong<sup>c</sup>, Bo-Hyun Kim<sup>a,\*</sup>, Seokwoo Jeon<sup>a,\*</sup>

**The water soluble GQDs were systematically characterized as a multiphoton fluorophore and cell imaging probes. When mouse primary hepatocytes were incubated with GQDs, no significant cytotoxicity was observed up to the treatment concentration of 100 µg/ml. Using these GQDs, mouse primary hepatocytes were successfully imaged by multiphoton fluorescence.**

Hepatocytes, the main tissue cells of the liver, are responsible for liver regeneration, detoxification, and the production of essential biochemicals.<sup>1</sup> The diagnostic imaging of hepatocytes without toxicity was developed in one of the fundamental interdisciplinary studies.<sup>2</sup> Recently, advances in the synthesis of nanomaterials have expanded biomedical imaging feasibility.<sup>3-5</sup> Inorganic nanoparticles engineered as nanoplatforams for effective imaging and targeted drug delivery have good stability, long term circulation, multi-functionality for imaging and therapy, and a high capability for drug delivery.<sup>6-8</sup> However, inorganic nanoparticles still need further improvements in refining process for reproducible synthesis, and to remove the remaining organic/inorganic passivation. Recently, carbon based nanomaterials are being considered as potential alternatives for use as bioimaging probes because of their fascinating optical properties and multi-functionality for imaging and drug delivery.<sup>4, 9, 10</sup> For example, carbon quantum dots functionalized by PPEI-EI have shown a two photon fluorescence under excitation of 800 nm and applied for tumour cell imaging.<sup>11</sup> Among allotropic forms of carbon based nanomaterials, graphene quantum dots (GQDs) have attracted considerable attention recently as a promising approach for biological labelling due to their chemical inertness, biocompatibility, low toxicity and high surface area.<sup>5, 9, 12, 13</sup> In recent studies, multiphoton induced fluorescence characteristics of GQDs have been reported and applied for imaging tumour cells, cellular and deep-tissue imaging,

and cell viability<sup>13-15</sup> However, due to defects and edge functional groups<sup>13, 16</sup>, which can act as bio-reactive sites and create clinical problems, a new synthetic process to develop GQDs is required.

Up to now, the application of water soluble GQDs for hepatocytes imaging, together with discussion of their cytotoxicity, has not been reported yet. Because primary hepatocyte has a physiological system generating basal metabolism like cells in living organisms, which is the difference from the tumour cell, if the GQDs could be used for positive control of tracking materials or gene delivery, the more precise studies for metabolism, drug-drug interaction, hepatotoxicity, transporter activity, and cell viability will be possible.

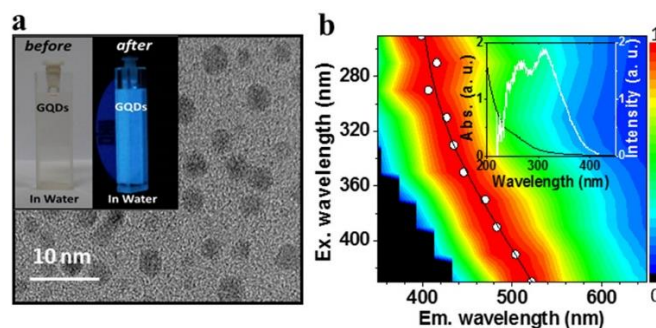


**Figure 1 a.** TEM image of GQDs. Inset. Before (left) and after (right) UV illuminated GQDs in water. **b.** 2D plot of PL spectra: Emission (Em.) wavelength vs. Excitation (Ex.) wavelength. Inset. UV-Vis absorbance (Abs.) and normalized PLE intensity of GQDs.

Here, we demonstrate the successful imaging of mouse primary hepatocytes using multiphoton luminescent GQDs, produced by the

water soluble synthesis of modified graphite intercalation compounds (GICs). For the cell imaging, their photoluminescence (PL) properties were measured by femtosecond pulse laser. We explored the cytotoxicity of the GQDs and applied them for the fluorescence imaging of mouse primary hepatocytes.

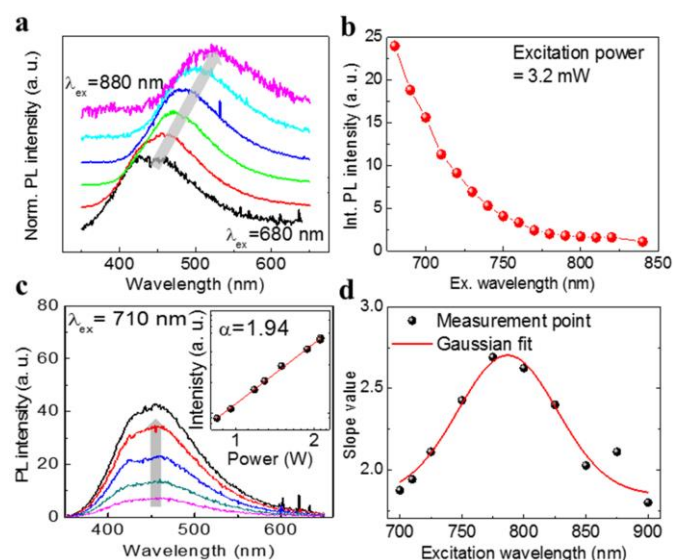
To control the defects and edge functional groups on GQDs, we have previously developed various methods, such as using a metal salts intercalated graphite compounds method<sup>17,18</sup>, diblock copolymer patterned method<sup>19</sup>, and hydrate salt intercalation system<sup>20</sup>. In this experiment, we adopted the method of modified graphite intercalation compounds (GICs) with hydrate salt to synthesize the GQDs.<sup>20</sup> In Fig. 1a, a transmission electron microscopy (TEM) image is shown which illustrates that most of the GQDs synthesized by the modified GICs with hydrate salt method have a size less than 10 nm. Moreover, the homogeneous blue luminescence shown in the inset of Fig. 1a suggests that the GQDs are not only well dispersed in water, but are also a blue fluorescent nanomaterial. The topological and chemical structures of GQDs were investigated by high resolution TEM, AFM, and FT-IR (Fig. S1). The results provide that GQDs have the high crystalline structure, ~1.0 nm layer thickness, and low epoxide functional groups, and are consistent with previous result<sup>20</sup>.

Figure 1b shows the luminescence characteristics of the GQDs. As the excitation wavelength ( $\lambda_{ex}$ ) of the GQDs is changed from 250 nm to 490 nm, the PL peak becomes red-shifted. However, the strongest PL intensity was observed at the emission wavelength ( $\lambda_{em}$ ) of ~400 nm ( $\lambda_{ex}$  ~310 nm) (Fig. S2a). The redshift of the PL peak can be attributed to variations of size, and to the defect or edge functionalized groups inducing emissive sites on the GQDs.<sup>16, 20-23</sup> In the PL excitation (PLE) measurement (Inset Fig. 1b), the PLE spectrum recorded at 400 nm shows two sharp peaks at ~266 nm and ~311 nm, which are most likely due to the  $\pi-\pi^*$  transition of the aromatic  $sp^2$  domains or the transition between bands induced mainly by the size effect, or the oxygen and defect states.<sup>16, 20, 22</sup> Figure S2b shows the PL decay profile fitted by double exponential with lifetimes of ~2.10 ns and ~7.88 ns. The faster decay was analysed to be the decay in the

intrinsic bandgap whereas the slow decay comes from extrinsic properties of the GQDs.<sup>20</sup> The quantum yield of GQDs excited by 310 nm at room temperature was about 4.0% (Fig. S1c).

Recently, Gan *et al.* and Ha *et al.* proposed that the shorter wavelength of PL in the GQDs is not caused by the upconversion via intermediate states but by multiphoton excitation via virtual intermediate states and it can be probed by pulsed-laser excitation.<sup>24, 25</sup> Accordingly, in this study we investigated the multiphoton induced PL of GQDs by using a home-built optical setup. A femtosecond Ti:sapphire pulse laser (80 MHz repetition rate, 140 fs pulse width) is used for multiphoton excitation.<sup>26</sup> In Fig. 2a, as the  $\lambda_{ex}$  increases from 680 nm to 880 nm, the upconversion PL peak red-shifted from 440 nm to 520 nm. However, intriguingly, under the same excitation power, the integrated PL intensity gradually decreases (Fig. 2b). These results are similar to the varying trend of single photon excited PL peak position and PL intensity (Fig. 1b and S2a). For further understanding of the multiphoton excitation of PL, the correlation of upconversion PL intensity with the excitation power was systematically investigated.<sup>27, 28</sup> The multiphoton excitation PL intensity measured at  $\lambda_{ex}$  = 710 nm linearly increased as the excitation power increased without significant change of spectrum shape (Fig. 2c). The integrated PL intensities showed that the multiphoton excitation PL intensity seemed to have quadratic proportional to the excitation power (slope ~ 1.94) (Inset Fig. 2c). In a series of investigations of the correlation between multiphoton excitation PL intensity and excitation power (Fig. S3), the integrated PL intensities for  $\lambda_{ex}$  in the range from 700 nm to 900 nm showed linear relations to the excitation power. The slope values dependence on the excitation power varied between 1.8 and 2.7 with Gaussian distribution (Fig. 2d). This suggests that synthesized GQDs have different multiphoton excitation properties under various excitation wavelengths. The GQDs show PL spectra excited by two or three photon when excited by the wavelength between 700 nm and 900 nm. This can be explained by two kind of the optical excitation levels of GQDs: One is intrinsic  $\pi-\pi^*$  transition of the aromatic  $sp^2$  domains and the other is the extrinsic transition between bands induced by mainly the size effect or the oxygen and defect states.<sup>20</sup> Consequently, the PL intensity of GQDs at near infrared frequency (from 700 nm to 900 nm) changes according to the dominant excitation level between intrinsic and extrinsic transitions. However, the energy difference between excitation and emission wavelengths was less than 1.2 eV which does not correspond to the variation of slope values. Therefore, although the PL of GQDs mainly occurs through the multiphoton excitation in the near infrared frequency, their radiative decay could occur in a band structure similar to single photon fluorescent materials.<sup>13, 29</sup>

Although carbon based nanomaterials can be used for biological applications, the cytotoxicity of GQDs has only been verified for limited cell lines.<sup>5, 9, 23</sup> Here, we evaluated the cytotoxicity of the GQDs with primary hepatocytes from the mouse using LDH detecting assay. Remarkably, the GQDs didn't impose a considerable toxicity to the hepatocyte cells up to 100  $\mu\text{g}/\text{mL}$  as compared to the controls (untreated,  $\text{CCl}_4$ , and EtOH) during 24 h incubation (Fig. 3a and S4). The experimental method for the LDH detecting assay is described in the Supporting Information. When we imaged the hepatocytes with an excitation wavelength of 790 nm under different concentrations of GQDs varying from 20  $\mu\text{g}/\text{ml}$  to 100  $\mu\text{g}/\text{ml}$  (Fig. 3b), the multiphoton excitation PL intensity increased as the concentration increased. Figures 3c and S5 illustrate the highly concentrated GQDs around the nucleus, that is, GQDs seems to mainly stain the cell body rather than the nucleus of the hepatocytes. The decrement of PL intensity during repeated



**Figure 2.** a. Normalized multiphoton PL spectra ( $\lambda_{ex}$  = 680 nm - 880 nm). b. Integrated upconversion PL intensities of GQDs with same excitation power. c. Upconversion PL spectra at various powers. Inset. PL intensity (I) vs. excitation power ( $P^n$ ). d. Slope values of PL intensity vs. excitation power.

imaging by multiphoton excitation (Fig. S6) was in the error range (Fig. 3d), suggesting that the photo-bleaching of GQDs by multiphoton excitation can be ignorable. Moreover, the GQDs show stability in the hepatocytes for two weeks (Fig. 3e and S7). This indicates that GQDs are a potential candidate probe for long duration high contrast bio-imaging.

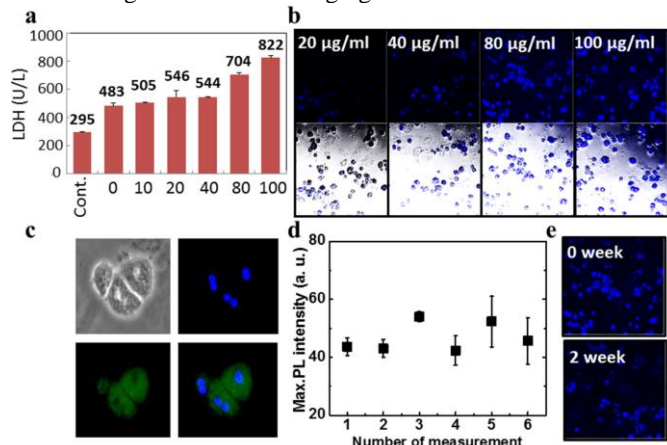


**Figure 3.** a. Cytotoxicity for mouse primary hepatocytes. b. Multiphoton images depending on GQDs' concentration. c. Mouse primary hepatocytes images with GQDs after 24 hours. Phase contrast image (top left), nucleus stained by DAPI (top right), green fluorescent GQDs (bottom left), and overlay image of DAPI and green GQDs (bottom right). d. Photo-bleaching test of GQDs by multiple (6 times) imaging. e. Imaging after 24 hrs (top) and after two weeks (down).

## Conclusions

We have demonstrated that the water soluble GQDs have multiphoton excited fluorescent properties and they can be used for imaging hepatocytes in the near infrared wavelengths. During the incubation and imaging of hepatocytes, the GQDs showed low cytotoxicity, low photo-bleaching and stability in the cells. Although further studies are indeed needed, our result suggests that the GQDs we have synthesized using modified GICs with hydrate salt have potential application as a bioimaging probe, and following edge functionalization, we expect them to be used for drug delivery to the liver.

## Acknowledgement

This research was supported by the grant (2011-0031630) from the Center for Advanced Soft Electronics under the Global Frontier Research Program of the Ministry of Education, Science and Technology, Korea, and Nano-Material Technology Development Program through the National Research Foundation of Korea (NRF) funded by the Ministry of Science, ICT and Future Planning (2013M3A6A5073173). It was also partially supported by the energy efficiency and resources of the Korea Institute of Energy Technology Evaluation and Planning (KETEP) grant funded by the Ministry of knowledge Economy, Korean government (No: 20122010100140).

## Notes and references

<sup>a</sup> Department of Materials Science and Engineering and Graphene Research Center of KI for the NanoCentury, Korea Advanced Institute of Science and Technology, Daejeon 305-701, Republic of Korea.

<sup>b</sup> Department of Physics Graphene Research Center of KI for the NanoCentury, Korea Advanced Institute of Science and Technology, Daejeon 305-701, Republic of Korea.

<sup>c</sup> Laboratory of Liver Research, Graduate School of Medical Science and Engineering, Daejeon, Republic of Korea.

Electronic Supplementary Information (ESI) available: [details of any supplementary information available should be included here]. See DOI: 10.1039/c000000x/

\* Corresponding author: bohkim@kaist.ac.kr or jeon39@kaist.ac.kr

1. S. Sherlock and J. Dooley, *Diseases of the liver and biliary system*, John Wiley & Sons, 2008.
2. L. H. Reddy and P. Couvreur, *J. Hepatol.*, 2011, **55**, 1461-1466.
3. D. P. Cormode, T. Skajaa, Z. A. Fayad and W. J. M. Mulder, *Arterioscl. Throm. Vas.*, 2009, **29**, 992-1000.
4. C. Q. Ding, A. W. Zhu and Y. Tian, *Accounts Chem. Res.*, 2014, **47**, 20-30.
5. S. J. Zhu, J. H. Zhang, C. Y. Qiao, S. J. Tang, Y. F. Li, W. J. Yuan, B. Li, L. Tian, F. Liu, R. Hu, H. N. Gao, H. T. Wei, H. Zhang, H. C. Sun and B. Yang, *Chem. Commun.*, 2011, **47**, 6858-6860.
6. G. Bao, S. Mitragotri and S. Tong, *Annu. Rev. Biomed. Eng.*, 2013, **15**, 253-282.
7. X. Michalet, F. F. Pinaud, L. A. Bentolila, J. M. Tsay, S. Doose, J. J. Li, G. Sundaresan, A. M. Wu, S. S. Gambhir and S. Weiss, *Science*, 2005, **307**, 538-544.
8. I. L. Medintz, H. T. Uyeda, E. R. Goldman and H. Mattoussi, *Nat. Mater.*, 2005, **4**, 435-446.
9. J. H. Shen, Y. H. Zhu, X. L. Yang and C. Z. Li, *Chem. Commun.*, 2012, **48**, 3686-3699.
10. S. C. Ray, A. Saha, N. R. Jana and R. Sarkar, *J. Phys. Chem. C*, 2009, **113**, 18546-18551.
11. L. Cao, X. Wang, M. J. Mezziani, F. Lu, H. Wang, P. G. Luo, Y. Lin, B. A. Harruff, L. M. Veca, D. Nurray, S. Y. Xie and Y. P. Sun, *J. Am. Chem. Soc.* 2007, **129**, 11318-11319.
12. H. J. Sun, L. Wu, W. L. Wei and X. G. Qu, *Mater. Today*, 2013, **16**, 433-442.
13. Q. Liu, B. D. Guo, Z. Y. Rao, B. H. Zhang and J. R. Gong, *Nano Lett.*, 2013, **13**, 2436-2441.
14. A. Pramanik, S. R. Chavva, Z. Fan, S. S. Sinha, B. Priya, V. Nellore and P. C. Ray, *J. Phys. Chem. Lett.*, 2014, **5**, 2150-2154.
15. J. Qian, D. Wang, F. H. Cai, W. Xi, L. Peng, Z. F. Zhu, H. He, M. L. Hu and S. L. He, *Angew. Chem. Int. Edit.*, 2012, **51**, 10570-10575.
16. K. P. Loh, Q. L. Bao, G. Eda and M. Chhowalla, *Nat. Chem.*, 2010, **2**, 1015-1024.
17. K. H. Park, B. H. Kim, S. H. Song, J. Kwon, B. S. Kong, K. Kang and S. Jeon, *Nano Lett.*, 2012, **12**, 2871-2876.
18. J. Kwon, S. H. Lee, K. H. Park, D. H. Seo, J. Lee, B. S. Kong, K. Kang and S. Jeon, *Small*, 2011, **7**, 864-868.



19. J. Lee, K. Kim, W. I. Park, B. H. Kim, J. H. Park, T. H. Kim, S. Bong, C. H. Kim, G. Chae, M. Jun, Y. Hwang, Y. S. Jung and S. Jeon, *Nano Lett.*, 2012, **12**, 6078-6083.
20. S. H. Song, M. H. Jang, J. Chung, S. H. Jin, B. H. Kim, S. H. Hur, S. Yoo, Y. H. Cho and S. Jeon, *Advanced Optical Materials*, 2014, **2**, 1016-1023.
21. G. Eda, Y. Y. Lin, C. Mattevi, H. Yamaguchi, H. A. Chen, I. S. Chen, C. W. Chen and M. Chhowalla, *Adv. Mater.*, 2010, **22**, 505-509.
22. D. Y. Pan, J. C. Zhang, Z. Li and M. H. Wu, *Adv. Mater.*, 2010, **22**, 734-738.
23. S. J. Zhu, J. H. Zhang, S. J. Tang, C. Y. Qiao, L. Wang, H. Y. Wang, X. Liu, B. Li, Y. F. Li, W. L. Yu, X. F. Wang, H. C. Sun and B. Yang, *Adv. Funct. Mater.*, 2012, **22**, 4732-4740.
24. Z. Gan, X. Wu, G. Zhou, J. Shen and P. K. Chu, *Adv. Optical Mater.* 2013, **1**, 554-558.
25. H. D. Ha, M.-H. Jang, F. Liu, Y.-H. Cho and T. S. Seo, *Carbon* 2015, **81**, 367-375.
26. F. Liu, M. H. Jang, H. D. Ha, J. H. Kim, Y. H. Cho and T. S. Seo, *Adv. Mater.*, 2013, **25**, 3657-3662.
27. H. H. Fan, L. Guo, K. F. Li, M. S. Wong and K. W. Cheah, *J. Am. Chem. Soc.*, 2012, **134**, 7297-7300.
28. C. Xu and W. W. Webb, *J. Opt. Soc. Am. B*, 1996, **13**, 481-491.
29. R. Hoffmann, *J. Am. Chem. Soc.*, 1968, **90**, 1475-1485.